A&A 409, 347–359 (2003)
DOI: 10.1051/0004-6361:20030995


Astronomy & Astrophysics

# The physico-chemical history of Falling Evaporating Bodies around $\beta$ Pictoris: The sublimation of refractory material

C. Karmann[1], H. Beust[1], and J. Klinger[2]

[1] Laboratoire d'Astrophysique de Grenoble, Université J. Fourier, BP 53, 38041 Grenoble Cedex 9, France
[2] Laboratoire de Planetologie de Grenoble, Université J. Fourier, BP 53, 38041 Grenoble Cedex 9, France

Received 20 December 2002 / Accepted 3 June 2003

**Abstract.** Transient spectral redshifted absorption events in the spectrum of $\beta$ Pictoris ($\beta$ Pic) have been attributed to comet-like bodies falling toward the star (*Falling Evaporating Bodies*, or FEB) and evaporating in its immediate vicinity. Dynamical models shows that these bodies originate from circular orbits at $\gtrsim$4 AU. After an eccentricity increase due to planetary perturbations, they end up as star-grazers. The physics of the cloud generated by the body's sublimation is highly influenced by the physico-chemical conditions inside the body. Thus it is necessary to investigate the composition and the behavior of the materials within the body in order to explain the observed features. The physico-chemical evolution of the bodies has been simulated during all the phases before and during their FEB state. First the fluctuations in the gas production rates of volatile solids in the first phase when the refractory materials have not yet evaporated has been studied. Later on, the refractory crust of the object evaporates even if the core still contains volatile solids. The simulation then shows a phase lag between the production rate of volatiles and of refractory materials during the periastron passage. The influence of dynamical and physical parameters on the FEB phenomenon are also investigated. We find that only a heterogenous population of bodies can produce all the absorption features that have been observed so far. These results are important for the understanding of the FEB phenomenon and can lead to a revision of the FEB sublimation model.

**Key words.** stars: individual: $\beta$ Pic – methods: numerical – comets: general – stars: circumstellar matter – stars: planetary systems: formation

## 1. Introduction

### 1.1. $\beta$ Pictoris

The dusty and gaseous disk surrounding the southern star $\beta$ Pictoris ($\beta$ Pic) (Smith & Terrile 1984) is considered today as a key example of a young planetary system in its early dynamical history, with an age of $10^7$–$10^8$ yr. Such kinds of systems are characterized by a large amount of dust that diffuses the stellar light. At the present stage of evolution, the primordial, optically thick disk has already been removed and the present disk is optically thin. It is known today that the dust we detect is not a remnant of this primordial disk, but rather composed of second generation material continuously replenished from inside the disk by larger, planetesimal-like bodies (see reviews by Artymovicz 1997; Vidal-Madjar et al. 1998; Lagrange et al. 2000).

*Send offprint requests to*: H. Beust,
e-mail: herve.beust@obs.ujf-grenoble.fr

### 1.2. Falling Evaporating Bodies and their chemical composition

Independent of disk imaging, transient spectral absorption events occurring in metallic lines have been monitored for several years around $\beta$ Pictoris (Vidal-Madjar et al. 1994; Lagrange et al. 1996). These events tend to vary on very short time-scales (days or even hours), and have been interpreted as resulting from the transit across the line of sight of sublimating star-grazing comet-sized bodies (*Falling Evaporating Bodies*, or FEBs). A model has been developed that reproduces the observed events (Beust et al. 1990, 1996, 1998) with many of their characteristics.

In spite of its ability to correctly explain the features observed, this earlier model is very sensitive to supposed physico-chemical properties of the evaporating bodies. Any change in chemical composition has an effect on the simulated spectral absorptions, both in terms of compared strengths of variable lines expected, and of dynamics of the corresponding species once escaped from the FEBs. In previous models, the assumption was that FEBs have the same chemical composition as Solar comets, i.e. refractory compounds having Solar relative composition abundances.

Direct measurements of the chemical composition of the variable features attributed to FEBs is not straightforward, as the depths of these components does not depend only on the abundance of the corresponding species, but also on the filling factor of the absorbing clouds in front of the stellar disk. It has been shown by comparison of variable features occurring in doublet lines that the absorbing material was mostly clumpy (Vidal-Madjar et al. 1994; Lagrange et al. 1996). Modeling (Beust et al. 1996) showed that the projected size of the ionic clouds escaping from the FEBs onto the stellar surface actually depends on the dynamics of the species they contain; moreover, the dynamics tends to differ from a given element to another (due to the variations in the sensitivity to radiation pressure). Consequently, measuring the chemical composition of FEBs from their spectral signatures cannot be performed independently of dedicated modeling. In this context, it has thus not been possible to heavily constrain the chemical composition of FEBs. All that can be stated today concerning refractory species, all what can be stated today is that Solar (i.e. cometary) composition is compatible with the observations and with the models within one order of magnitude. Conversely, the composition of the stable circumstellar gas is better constrained (Lagrange et al. 1998), with the result that refractory species indeed have Solar relative composition. If we assume this stable gas also to be linked to FEBs (because it needs to be permanently refilled; see Lagrange et al. 1998), then we may suppose that this also applies to the chemical composition of the FEBs themselves.

### 1.3. The initial composition of the Falling Evaporating Bodies

The present work is the continuation of work published by Karmann et al. (2001, hereafter K01). In that paper we focused on the quantity of volatile materials contained in the object and we developed a model of the evolution of FEB progenitors and simulated the first phase of their life, when they stayed on circular orbits. It turned out that FEB progenitors are probably not icy in the major part of their volume. Depending on the age of $\beta$ Pic, the size of the object, and the distance to the star, it can be either free from ice, or composed of a small mixed dust-ice core surrounded by a thick refractory crust. This result was very important; indeed in previous work we had always assumed that those bodies should be made of mixed dust and ices without any differentiated structure, and part of the evaporation model was based on this assumption.

Because of the lack of ice in the object, this evaporation scenario needed to be revised. Indeed, volatile compounds (dissociated water, CO) were assumed to be released by the FEBs with cometary abundance, i.e. with an abundance roughly equal to that of the refractory compounds. As the volatile species mostly do not feel an intense radiation pressure from the star, they were supposed to play the role of retaining the metallic ions in the vicinity of the nucleus. If the ice is restricted to a small core in the object, the scenario becomes more complicated. We have to know if some volatile material can leave the object during the sublimation, and how much. In fact, in our work, we have focused on the relative amount of volatile or refractory material that is evaporated during the FEB phenomenon. In Sect. 2, we roughly describe the method used and focus on the improvements made to simulate the sublimation of refractory materials. In Sect. 3, we study the first phase of the evolution of the body, when the eccentricity of the object progressively grows so that heliocentric distances can be reached were the refractory compounds begin to sublimate. In Sect. 4, we present the results concerning the evaporation of the refractory crust, and in Sect. 5 the evaporation of the remaining nucleus. The role of a dust cloud around the object is discussed in Sect. 6. Finally, in Sect. 7, we investigate the influence of the model parameters on the production and on the lifetime of the object, and in Sect. 8, we present the implications of this study for our present knowledge of the FEB evaporation process. Our general conclusions are presented in Sect. 9.

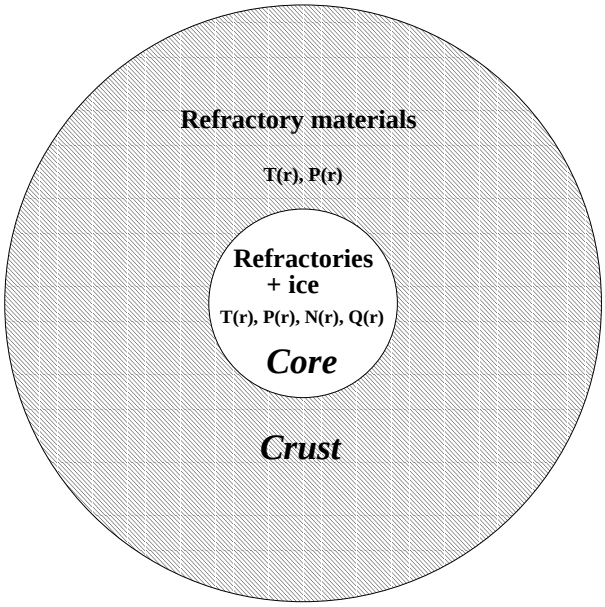


**Fig. 1.** Structure of a FEB. During the simulations, the evolution of functions $T(r,t)$, $P(r,t)$, $N_i(r,t)$ as well as the sublimation rates of the object are computed.

## 2. The method

The method was described in K01. Here we summarize it and describe its evolution since that time.

### 2.1. General assumptions

Based on the results of K01, we can now say that FEB most likely originate from more or less circular orbits at 4 to 5 AU from the star and that their surface is likely to be covered by a thick, refractory crust.

The FEB is considered as a porous sphere of matter, composed of a refractory crust and a core of mixed ice and refractories (see Fig. 1). The object is trapped in a mean-motion resonance with a Jupiter-sized planet. Its orbit will undergo a secular evolution that brings it from a nearly circular to a star-grazing orbit. Therefore, differently from K01, where we

investigated the equilibrium on a circular orbit at a given distance to the star, we need to consider here orbits that are far from circular. We thus need to compute at every step the radiation flux received from the star. We no longer consider the dust as inert matter, and compute its sublimation at the surface. Nevertheless, as this sublimation occurs only in a zone close to the star, at 0.4 AU (Beust et al. 1998), we still assume that the refractory sublimation rate is equal to zero at distances greater than 0.4 AU. Also, as shown by the simulations, most of the dust sublimation occurs at the surface of the object, since only the surface layers reach sufficiently high temperatures at periastron; as a consequence, we assume the dust as completely inert inside the object. In order to reduce the complexity of the model, other phenomena such as fragmentation of the body have not been considered. As in K01, the object is considered as a "fast rotator". In some cases, a "synchronous rotator" has also been considered.

### 2.2. Dynamical evolution

In order to simulate the evolution of the internal physical processes of the object, we have to know at any moment its distance to the star. We must therefore simulate the mouvement of the object on its orbit and the secular evolution of the orbit. However, this dynamical evolution is not the topic of our study, so we will not go into detail in this article. The dynamical evolution of a FEB is described and discussed by Beust & Morbidelli (1996, 2000). All we need to know here is that the orbital eccentricity of the object is subject to a gradual increase that brings it to $\sim$1 within $10^5$–$1.5 \times 10^5$ yrs. In order to render our simulation self-consistent, we recompute here this secular evolution together with the physical behavior of the body. For the purposes of dynamical evolution, the body is taken as a mass-less particle in a mean-motion resonance with a Jovian-like planet; its motion is integrated with a classical 4th order Runge-Kutta integrator with adaptative time-step. Many parameters can influence the dynamics of the object, and therefore the quickness of the growth of the eccentricity of the orbit:

- the order of the resonance (3:1 or 4:1);
- the initial eccentricity of the object;
- the mass ratio between the Jovian planet and the star;
- the eccentricity of the planet's orbit;
- the semi-major axis of the orbit.

All these parameters are integrated into the simulation and are the subject of a specific comparative study.

### 2.3. Physical model

The main physical process involved in our model is the phase transition of volatiles and refractories. Initially, the material is considered to be in thermodynamical equilibrium. Most of the time, inside the object the gas is close to saturation and so automatically compensates for local loss or gain of gas due to gas diffusion towards the surface or the interior. At the surface, we have free sublimation with an external pressure equal to zero.

The evolution of temperature and pressure inside the object is constrained by a set of equations involving the heat equation and the gas diffusion equation. The heat transported by the gas that diffuses throughout the matrix, i.e., the sensitive heat, is computed as a source term in the heat equation. The mode of diffusion of the gas is always the Knudsen mode, as it has been confirmed a posteriori by the simulations. The new feature taken into account here is the erosion at the surface when the refractories sublimate. This erosion is computed at each step as follows:

$$\frac{\mathrm{d}r}{\mathrm{d}t} = \frac{\mathrm{d}r}{\mathrm{d}V}\frac{\mathrm{d}V}{\mathrm{d}t} = -\frac{1}{4\pi r^2}\frac{Q_\epsilon(t)}{\rho_i} \cdot 4\pi r^2 = -\frac{Q_\epsilon(t)}{\rho_i} \,, \tag{1}$$

where $r$ is the radius of the object, $V$ the volume, $Q_\epsilon(t)$ the sublimation rate at the surface (mass loss per surface unit and unit of time). $\rho_i$ represents the mass concentration of species $i$ (mass per unit volume, taking into account the porosity). Therefore, the reduction of the radius of the object at a given instant is directly proportional to the sublimation rate at the surface.

### 2.4. Numerical resolution

Because of the spherical symmetry of the object, we can discretize it into concentric shells of equal depth d$r$. The system of equations of our model is solved by numerical integration for specified boundary conditions. The scheme used at each time step is a Douglas-Jones predictor- corrector scheme (Douglas & Jones 1963), which has the advantage of being stable and simple to use.

In order to have a good accuracy in the places where the sublimation occurs, we have chosen dr within the range of 10 cm to 1 m. The drawback of this uniform spatial discretization is that we ended up with a huge number of shells where the temperature and pressure values had to be computed at each time step. This takes a lot of time, even on a modern computer. This problem has been solved when we noticed on the first simulations that the main physical processes occurs in small regions of the object: at the interface between its core and its crust. Therefore we grouped the shells in the regions far from the surface and the interface between the crust and the core, where pressure and temperature were supposed to evolve linearly with $r$. By doing this, we have multiplied the efficiency of the code by a factor of several hundred.

### 2.5. Physical and dynamical parameters

We take the same parameters as in K01 for ice, albedo and thermal emissivity of the object. The refractory matter is represented by only one species, the thermal characteristics, density and sublimation rate of which are taken from the literature. Most of the time we consider obsidian which is a relevant choice according to what is observed in the Solar System, and which is generally used (Draine & Lee 1984), but we also investigate the influence of a less volatile refractory species (graphite) and a more volatile one (magnetite). The characteristics of all material used are taken from the literature. The values used and the corresponding references are listed in Table 2 from Beust et al. (1998). For a typical run, the object is considered to be trapped in a 4:1 mean-motion resonance with a planet having a mass of 0.001 of the mass of the star, and an eccentricity

**Table 1.** Parameters used for a typical run of our sublimation.

| | |
|---|---|
| $\mu = M_{\rm pla}/M_*$ | 0.001 |
| Radius | 10 km |
| Refractory material | obsidian |
| Refractory/volatile mass ratio | 1 |
| Porosity | 0.8 |
| Semi-major axis value | 4 AU |
| **For a 4:1 mean-motion resonance:** | |
| Initial eccentricity | 0.1 |
| Eccentricity of the planet | 0.07 |
| **For a 3:1 mean-motion resonance:** | |
| Initial eccentricity | 0.2 |
| Eccentricity of the planet | 0.1 |

of 0.07. The initial orbit of the object has an initial eccentricity of 0.1. We also tested objects trapped in 3:1 mean-motion resonance, with an initial eccentricity of 0.2, and an eccentricity of the planet of 0.1 (see Thébault & Beust 2001 for justification). For clarity, all the parameters are listed in Table 1. The influence of most of the parameters will be investigated in Sect. 7.

## 3. First phase: The eccentricity growth up to the refractory sublimation limit

### 3.1. Description

Initially, the FEB is on a quasi-circular orbit in a mean-motion resonance. Its eccentricity then grows to nearly 1 in $\sim 10^5$ yrs. We define the first phase of this evolution as the time span when the periastron of the orbit is far enough from the star so that the object never enters the zone where refractories undergo sublimation (this zone is defined here as $\gtrsim$0.4 AU from the star). Therefore, only sublimation of volatile materials (ices) occurs.

The simulations describe the evolution of the production rates of volatiles of the object. In this evolution we can distinguish two kinds of variations. The first and more obvious variation is a regular oscillation of the sublimation rate on a time scale equal to the orbital period of the body, as shown in Fig. 2. It follows the motion of the body along its orbit, but surprisingly, the sublimation rate is larger at apoastron, and smaller at periastron; one would indeed expect that the production rate of the nucleus should be larger at periastron.

This apparent paradox is due to the damping of the heat wave by the crust of refractories. When the crust reaches a thickness of at least 100 m, the core does not see any change in the heat flux coming from the surface on the time scale of one orbital period. Therefore the temperature at the core is almost constant on this time scale, leading to an approximately constant sublimation rate of volatiles at the interface between the core and the refractory crust.

Then, the quantity of gas released by the object is entirely controlled by the diffusion of the gas through the surface. The gas outflow is smaller when the temperature is higher (K01, Eq. (11)). Therefore, at periastron the gas diffuses less easily through the upper part of the crust, and the production rate becomes smaller. The second variation occurs on the time scale

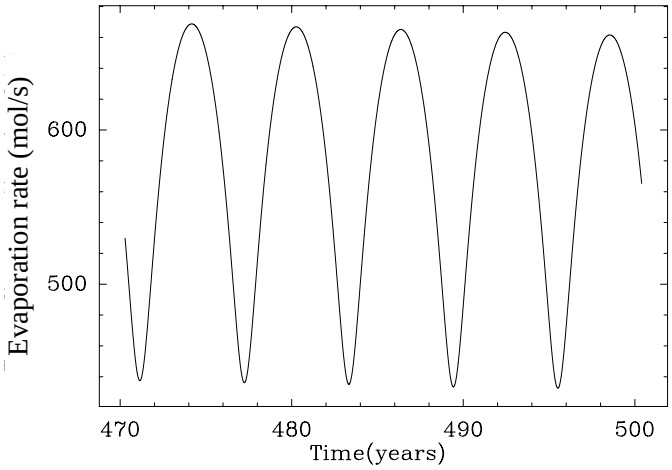


**Fig. 2.** Evolution of the sublimation rate of the volatiles at the surface over a few revolutions, when the object has an eccentricity equal to 0.4. The minima of the curve correspond to the periastron passages, and the peaks to the apoastron passages

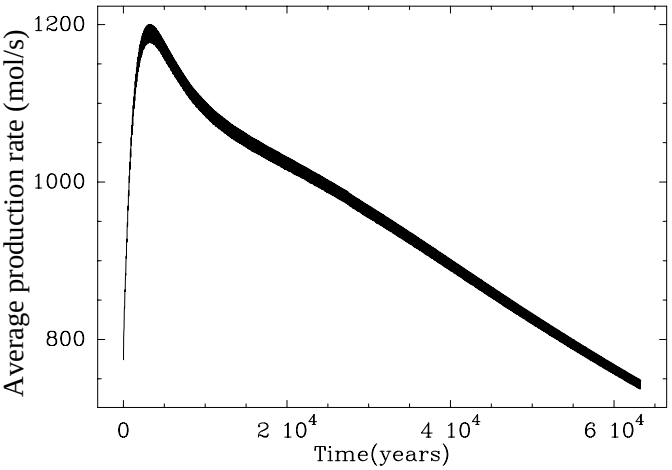


**Fig. 3.** Evolution of the sublimation rate of the volatiles at the surface averaged over the evolution of the orbit, when the eccentricity of the object grows from 0.05 to 0.9. The rapid growth of the computed rate at the beginning of the evolution matches the evolution of the simulated object towards its equilibrium.

of the evolution of eccentricity. It shows up when we average the production rate along the orbit, for relatively thin crusts (7–8 km) (Fig. 3). As the eccentricity increases, the mean sublimation rate of volatiles decreases. This time the sublimation rate is directly related to the production at the core. The crust is therefore not sufficient to average the wave of heat. The sum of energy received by the object along one orbit is calculated by integrating the radiation flow received from the star over this period of time:

$$\begin{aligned} E &= \int_0^T \frac{FR_*^2 \cdot \mathrm{d}t}{d_*^2} \propto \int_0^T \frac{\mathrm{d}t}{d_*^2} \propto \int_0^{2\pi} \frac{\mathrm{d}\nu}{d_*^2}\frac{\mathrm{d}t}{\mathrm{d}\nu} \\ &\propto \int_0^{2\pi} \frac{\mathrm{d}\nu}{d_*^2}\frac{(1-e^2)^{3/2}}{(1+e\cos\nu)^2} \propto (1-e^2)^{3/2}\int_0^{2\pi}\frac{\mathrm{d}\nu}{d_*^2(1-e\cos\nu)^2} \\ &\propto (1-e^2)^{3/2}\int_0^{2\pi}\frac{\mathrm{d}\nu}{a(1-e^2)}, \end{aligned} \quad (2)$$

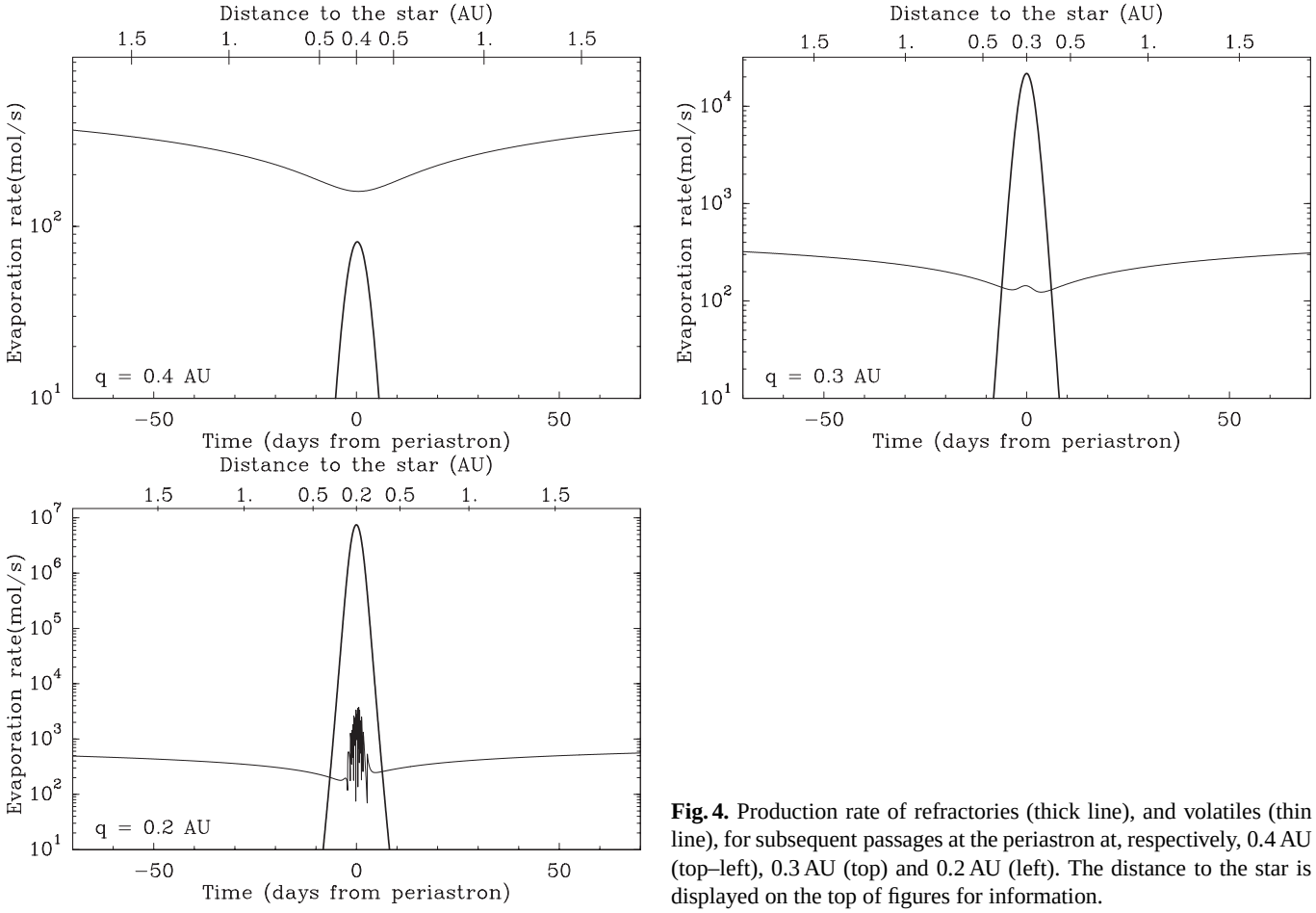


**Fig. 4.** Production rate of refractories (thick line), and volatiles (thin line), for subsequent passages at the periastron at, respectively, 0.4 AU (top–left), 0.3 AU (top) and 0.2 AU (left). The distance to the star is displayed on the top of figures for information.

where $F$ is the radiation flux at the stellar surface, $R_*$ is the radius of the star, $d_*$ the distance to it, $T$ the orbital period, $\nu$ the true anomaly, and $a$ the semi-major axis. Finally

$$E \propto \sqrt{1-e^2}. \tag{3}$$

The energy recieved is therefore a decreasing function of the eccentricity. Basically, when the eccentricity is high, the body undergoes a stronger radiation flux at periastron, but also a weaker one at apoastron. By virtue of Kepler's second law, the object spends more time at apoastron, so that the latter effect is dominant.

For very thick ($\gtrsim$8 km) crusts (and consquently very small cores), this evolution is not so obvious. The sublimation rate is almost constant over this phase. This means that the crust is then sufficiently large to average the temperature wave over a time period of $10^5$ yrs.

## 4. Second phase: The sublimation of the refractory crust

### 4.1. Description

The second phase of evolution begins when the object enters the refractory-sublimation zone on a part of its orbit. At this moment it becomes a potentially observable Falling Evaporating Body.

In this phase, the refractory crust of the object is progressively sublimated, as volatiles continue to diffuse through it towards the surface. The simulations have been used to study the production rate of this material. The results are shown in Fig. 4. The production of refractories always shows a sharp peak at periastron. This peak becomes considerably greater as the periastron gets closer to the star. For large periastron values (~0.4 AU), it remains significantly smaller than the production of volatiles, even if the production rate reaches a minimum at periastron, as explained above. At somewhat intermediate periastron values (~0.3 AU), the sublimation of refractories now overcomes that of volatiles at periastron, even if now the production of volatiles exhibits a little peak during the periastron passage. For small periastron values (~0.2 AU), the production of refractories is by far the dominant phenomenon at periastron, while the production rate of volatiles jumps by one order of magnitude at the same time. The peak of volatiles at periastron is due to the quantity of volatile gas which is contained by the refractory material before its sublimation. If that refractory matrix disappears, then an important amount of volatile gas is suddenly released. It is important to notice that this production is far weaker than the production of refractories, as long as the crust has not disappeared, and still protects the core from sublimation.

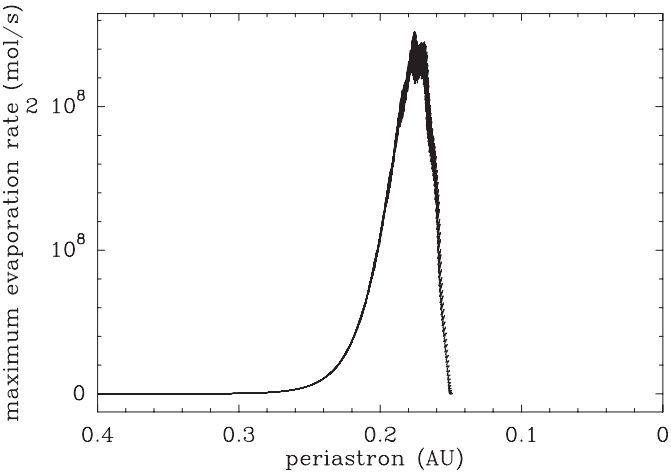


**Fig. 5.** Sublimation rate of refractories at each periastron for a single object.

### 4.2. Simplified model

The study of the energy balance at the surface shows that we can safely ignore at this time the heat exchanges between the surface and the interior of the body. Indeed, when the refractory sublimation zone is reached, the temperature of the surface goes to very high values (from 1400 K to more than 2200 K). Mathematically we can see that, as the surface sublimation rate is an exponential function of a polynomial in $T$, and as the thermal reemission is proportional to $T^4$, these two processes rapidly become predominant to heat conduction towards the inside of the body, which can be approximated as proportional to $T$.

Therefore we can build a simplified model of the surface of the object where its interior is ignored, and the heat balance only involves the two processes mentioned above and the heating by radiation flux from the star. This way, we can easily compute how much refractory material is evaporated, and how the body's size is reduced.

Figure 5 displays the sublimation rate of the refractories at each periastron in the framework of this simplified model. We can see that the main part of the sublimation takes place over a small range of periastron values. At too large distances, the temperature is too low to evaporate a great quantity of materials, and at small distances, the object becomes too small. An important point is that, with standard parameters, the object disappears very quickly. As a general rule, the body can hardly go to a periastron smaller than 0.1 AU. This result is essential for the interpretation of the FEB phenomenon. From observational characteristics, it was convenient to classify the observed spectral variation towards $\beta$ Pic in 3 subsets (Beust et al. 1998): VLVFs (Very Low Velocity Features), LVFs (Low Velocity Features), and HVFs (High Velocity Features). This distinction appeared to be related to the distance of the body to the star when it crosses the line of sight. HVFs correspond to the closest periastron passages, and are only consistent with periastron values $\lesssim$0.1 AU. HVFs are actually less frequent than LVFs and VLVFs, but they are still commonly observed features.

In the core, the sublimation of volatiles remains weak as long as a crust is still present, even when it has become very thin. Therefore the size of the core is not reduced very fast by sublimation, and at the end, the surface of the object meets the sublimating surface of the core. Then the third phase begins, described in Sect. 5. This result was not intuitive: one could have thought that the core should disappear before the crust, or that the crust would always have a minimal size, but this is not the case. This is mainly due to the fact that the major part of the heat received by the object is used for the sublimation on the surface, without affecting the core.

## 5. Third phase: The sublimation of the nuclei

### 5.1. Description

As long as the FEB undergoes periastron passages, it loses some matter at its surface, and its size progressively decreases. If the object still contains an icy core, the study described in Sect. 4 shows that there is a time when the crust surrounding this core disappears completely, and when the core reaches the surface. The moment when this happens is constrained by the initial size of the crust. However, as we have shown before, the size of the core is small, so it is likely that the surface of the object reaches the surface of the core near the end of its evolution, and this is what we observe in our runs. For an obsidian-filled FEB of 10 km and with a core of radius 4 km, the core disappears at a periastron of roughly 0.18 AU. The periastron value corresponding to this event is not very sensitive to the parameters of the simulation, (except for the refractory material, for which the parameter values are dramatically important. We will focus on this in Sect. 7.2.1). After this, the FEB enters its last phase, where the core undergoes free sublimation at the surface, and therefore produces considerably more volatiles. Let us discuss first what is occurring between two periastrons. When the object leaves the refractory sublimation zone, the core continues to sublimate volatiles, and it is possible that a new crust forms during the few years preceding the next periastron. Three questions then arise:

- What will the thickness be of this crust?
- Will it disappear at the next periastron?
- What consequence does it have on the production of refractories and volatiles at the passage to the next periastron?

Recall that the orbital period of our objects trapped in a mean-motion resonance at 4 AU is around 6 years. The passage at the periastron, in the refractory sublimation zone, lasts only around 10 days, and therefore is considerably shorter. So it is likely that a temporary crust would form between two periastrons. Our simulations can give the answer of whether the object is likely to disappear during the following periastron. The simulations have been used to observe the evolution of the radius of the object and the radius of the core during this phase and the preceding one. This evolution is shown in Fig. 6. The left panel confirms that the core, in the crust sublimation phase, does not shrink very much. Then, when the crust has disappeared, the radius of the object and that of the body become identical.

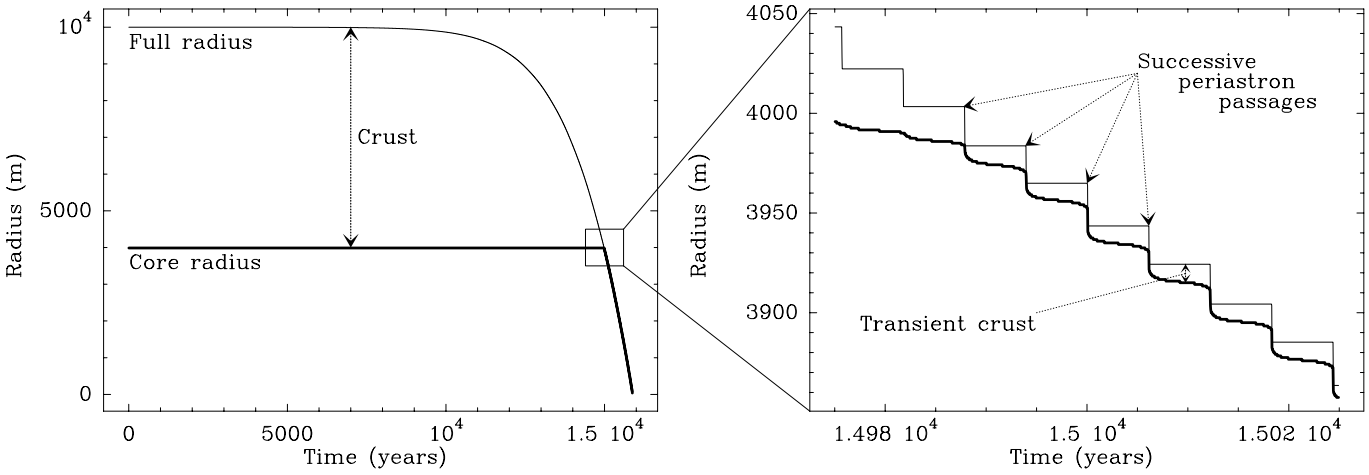


**Fig. 6.** Evolution of the radius of the object and of the core, along with the passages at the periastron, for an object with an initial core radius of 4 km, and an initial object radius of 10 km (and therefore an initial crust depth of 6 km). The right panel shows what is going on when the crust disappears. Between two successive periastrons, a small crust takes form, the size of which is a few meters. The particular "stair" shape of the evolution of the radius of the core is not physical: it is a numerical artifact, due to the discretization of the radius in the simulation. Still, the general form of the curve is still reliable, as it is consistent with what we obtain when we increase the spatial accuracy of the simulation.

The new crust that appears then will be very small, with respect to the size of the object.

The right plot of Fig. 6 focuses on the beginning of this simultaneous sublimation phase. It shows the evolution of the radius on a few successive orbits. The radius of the body is a monotoneously decreasing curve, which drops by a few meters at each passage at periastron. The evolution of the radius of the core is more irregular. First, it shrinks a little when the original crust is still present. When the thickness of the crust is reduced to a few meters, the sublimation of volatiles is accelerated. Then we see that each time the radius of the object reaches the radius of the core, i.e. when the refractory crust disappears completely, the core radius follows, as the core radius cannot be greater than the radius of the object. Then we have a simultaneous sublimation at each periastron passage. The depth of the crust depends on a few parameters, the most significant being the semi-major axis of the orbit, which constraints the period between two periastrons and the average distance along the orbit. For the value at 4 AU that we have assumed (and therefore for an orbital period of 6 years) the crust has a size of $3.7 \pm 0.5$ m. This temporary crust is therefore very small, with respect to the actual size of the body, but it is important as we will see below, even if it disappears very fast. Note that this crust disappears at each periastron: the sublimation of refractories is soon sufficiently strong to sublimate more than 4 m of crust at each periastron passage. The production rates of volatiles and refractories along one orbit are shown in Fig. 7. In the first plot we see what happens during the periastron passage. We see that the production rate of volatiles diminishes progressively after a passage at the periastron. This is evidence for the apparition of a new crust. At each periastron, while the crust disappears, the volatiles sublimation rate grows considerably. The second plot confirms this fact. It also shows that at the periastron passage, the volatile sublimation rate becomes similar to the refractory sublimation rate multiplied by a factor that is the ratio in the core of the quantity of refractory matter to the quantity of volatile matter. This is in contrast with the previous phase where the object was sublimating a quantity of refractories considerably greater than the quantity of volatiles.

The third figure shows what is going on at the passage of the periastron. The peaks of the production rates of volatiles and refractories are present, and we can notice that there is a time delay between them, the refractory one appearing before the volatile one, and disappearing before too. This delay in the apparition of the volatile peak is directly linked to the time necessary to sublimate the new crust that formed since the last passage at the periastron. When the new crust is evaporated, then the volatiles undergo a free sublimation. Also, the decrease of the volatile production rate occurs later because it needs some time to create a new crust. It is a long process, so the decrease of the volatile production rate is slower than the decrease of the refractory production. We can identify three phases during a passage at a periastron: the first one when the sublimation of refractories dominates, the second one when both production rates are of the same order, and the third one when the sublimation of volatiles dominates. Therefore, the existence of the crust induces a disymmetry of the sublimation process with regard to the periastron passage, a seasonal effect that potentially has a great incidence on the observations of the FEB phenomenon.

The simulations also show the transition between this phase and the previous one, at the level of the production rate. Figure 8 shows the two production rates at the periastron passages as the periastron distance decreases. The evolution curve of refractories has been described in the previous phase: it grows considerably as the periastron value decreases, and falls as the object becomes small. This is due to the fact that the sublimation surface has considerably decreased. The volatile sublimation rate is first very small and constant. It grows progressively while remaining small as the thickness of the crust decreases. Then it jumps abruptly when the crust disappears. Then it follows the same evolution as the production rate of refractories, decreasing with the sublimation surface. The ratio

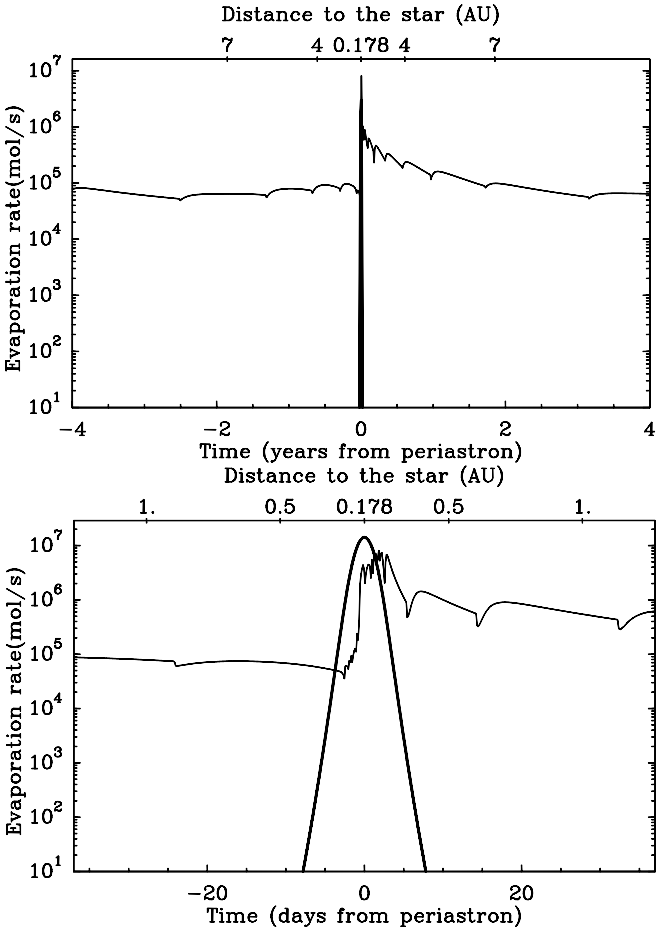


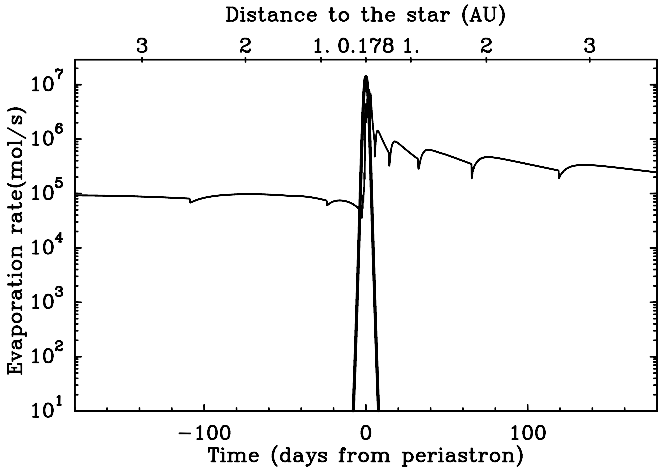


**Fig. 7.** Sublimation rate of refractory matter (thick line), and of volatiles (thin lines), along an orbit, when the surface reaches the core. The periastron of the FEB is 0.178 AU. From one plot to another, we focus on the details of the periastron passage. The small "bumps" of the volatiles's curve is due to a numerical artifact, related to the discretization of the radius in the simulation. Still, the general form of the curve is still reliable, as it is consistent with what we obtain when we increase the spatial accuracy of the simulation.

between the two sublimation rates is there the same as the ratio of the dust mass to the mass of ice in the core.

## 6. The role of the dust

A question that may be asked of our model is whether the production of dust by the FEB could affect the results. In Solar comets, the dust production is triggered by the evaporation of volatiles through its surface. We may expect this process to be present in our FEBs. The situation may be different depending whether refractory material evaporates or not. When only the volatiles evaporate, the preceding results show that the presence of a dust coma around the nucleus should not drastically affect the evaporation rate of volatiles. As a matter of fact, an optically thick dust coma surrounding the nucleus is basically equivalent (as seen from the inner volatile core) to a body with a larger radius. The evaporation rate of volatiles appeared not to depend on the radius of the surrounding refractory matrix. Hence we should expect the role of the dust to be minor.

When refractory material evaporates, it occurs at the surface. An optically thick dust cloud may stop dust sublimation at the surface, displacing it to the outer edge of this cloud. We need to estimate the size of this cloud. Suppose that dust is produced at the surface of the FEB. For simplicity we consider that all dust grains have the same radius $s_0$ (typically 0.1–1 $\mu$m) and that the dust cloud expands spherically with a constant velocity $v_e$ (typically 1 km s$^{-1}$). If $Q_{\rm dust}$ is the dust production rate per unit of surface at the level of the nucleus, then the dust density at distance $d$ to the nucleus is

$$\rho = \frac{r^2 Q_{\rm dust}}{d^2 v_e}, \quad (4)$$

where $r$ is the radius of the body. If the dusty particles do not sublimate and keep expanding radially, then we showed in

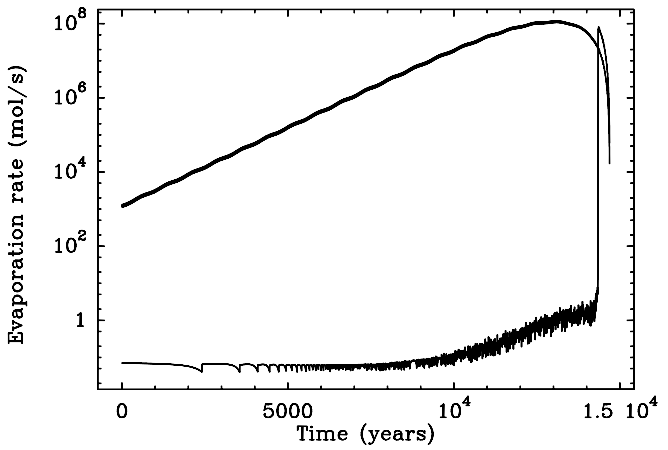


**Fig. 8.** Evolution of the production rate at each periastron passage for refractories (top curve) and volatiles (bottom curve), during the last moments of the FEBs life. Refractories are dominant until the complete sublimation of the crust, where the strong growth of the volatiles production occurs.

Beust et al. (1990) that the optical depth generated by these grains should read

$$\tau = \frac{3Q_{\rm dust} r^2}{4 s_0 \delta v_e} \frac{\theta}{d \sin\theta}, \quad (5)$$

where $\theta$ is the tilt angle with the nucleus – star direction, and $\delta$ is the density of the dust particles. In this condition, constant optical depth surfaces are parabolic-like surfaces around the nucleus, verifying the polar equation

$$d = \frac{\theta}{\sin\theta} d_0, \quad (6)$$

where $d_0$ is the distance in the nucleus – star direction. We expect dust sublimation to occur at the level of such a surface, typically the one corresponding to $\tau = 1$.

When dust production is triggered by volatile sublimation, we may expect that the gas to dust production mass ratio is close to unity. Assuming this and the above quoted maximum volatile production rates ($\sim 10^7$ mol/s), we find that for $\tau = 1$, $d_0$ ranges typically between 100 and 1000 km. This is very small compared to the star and the size of the orbits, and validates the hypothesis of spherical symmetry. $d_0$ is nevertheless significantly larger than the nucleus. Hence we might expect dust sublimation not to occur at the surface of the FEB.

As we consider that the dust is not evaporated, this estimate must be considered as an upper limit. In a more realistic description, we may consider that the sublimation of dust occurs along a surface with polar Eq. (6). This surface will be subject to erosion due to dust evaporation, that we will describe as a variation of the characteristic size $d_0$. The decrease of $d_0$ is due to the sublimation of dust along the surface. It may be slowed by the arrival of fresh dust coming from inside as a result of the spherical expansion. Consider a circular layer in this surface of thickness d$\theta$ at tilt angle $\theta$. The mass sublimated within d$t$ is

$$\mathrm{d}M_{\rm subl} = 2\pi d^2 \sin\theta Q_{\rm s} \mathrm{d}\theta = 2\pi d_0^2 Q_{\rm e} \frac{\theta^2}{\sin\theta} \mathrm{d}t, \quad (7)$$

where $Q_{\rm e}$ is the surface sublimation rate of the refactory material given in K01 (which depends only on the temperature). The mass that flows through the surface due to spherical expansion is given by:

$$\mathrm{d}M_{\rm flow} = 2\pi r^2 \rho v_{\rm e} \sin\theta \cos\phi \, \mathrm{d}t, \quad (8)$$

where $\phi$ is the angle between the outflow velocity and the normal to the surface. After some algebra, we derive

$$\mathrm{d}M_{\rm flow} = \frac{2\pi r^2 Q_{\rm dust} \theta \sin^2\theta}{\sqrt{\theta^2 + \sin^2\theta - 2\theta \sin\theta \cos\theta}} \mathrm{d}t. \quad (9)$$

If after d$t$, the dust sublimation surface has moved by d($d_0$), the total mass balance will be

$$\mathrm{d}M_{\rm balance} = 2\pi\rho d^2 \sin\theta \left(\frac{\mathrm{d}(d)}{\mathrm{d}(d_0)}\right) \mathrm{d}(d_0) = \frac{2\pi r^2 \theta Q_{\rm dust}}{v_{\rm e}} \mathrm{d}(d_0). \quad (10)$$

We must also have

$$\mathrm{d}M_{\rm balance} = -\mathrm{d}M_{\rm subl} + \mathrm{d}M_{\rm flow}. \quad (11)$$

After simplification, this gives us a differential equation for $d_0$ as:

$$\frac{1}{v_{\rm e}} \frac{\mathrm{d}(d_0)}{\mathrm{d}(d_0)} = -\frac{Q_{\rm e}}{Q_{\rm dust}} \frac{d_0^2}{r^2} \frac{\theta}{\sin\theta} + \frac{\sin^2\theta}{\sqrt{\theta^2 + \sin^2\theta - 2\theta\sin\theta\cos\theta}}. \quad (12)$$

Along the nucleus – star axis, characterized by $\theta = 0$, the equation reduces to

$$\frac{1}{v_{\rm e}} \frac{\mathrm{d}(d_0)}{\mathrm{d}t} = 1 - \frac{Q_{\rm e}}{Q_{\rm dust}} \frac{d_0^2}{r^2}. \quad (13)$$

This equation has the following solution

$$d_0(t) = d_{0,\rm final} \tanh\left(\frac{t + K}{t_{\rm c}}\right), \quad (14)$$

with

$$d_{0,\rm final} = r\sqrt{\frac{Q_{\rm dust}}{Q_{\rm e}}} \quad \text{and} \quad t_{\rm c} = \frac{r}{v_{\rm e}} \sqrt{\frac{Q_{\rm dust}}{Q_{\rm e}}}. \quad (15)$$

In this equation $K$ is a constant fixed by the initial conditions; $d_{0,\rm final}$ is the final equilibrium value for $d_0$ and $t_{\rm c}$ is a characteristic time for reaching it.

Of course this description holds only if $d_{0,\rm final} > r$, i.e. if $Q_{\rm dust} > Q_{\rm e}$. If this is not the case, then $d_0$ decreases down to the surface of the FEB and no dust cloud is able to survive. The sublimation is too efficient to let a dust cloud expand. This situation appears to occur in most of our simulations, as we assume that $Q_{\rm dust}$ should be roughly equal to the production rate of volatiles. In the second phase (Fig. 4), $Q_{\rm dust} > Q_{\rm e}$ as soon as the FEB is closer to the star than $\sim$0.35 AU. In the third phase, only after periastron (Fig. 7) may we have $Q_{\rm e} > Q_{\rm d}$, but only by a factor less than 10. This gives $d_{0,\rm final} \lesssim 3R$ and $t_{\rm c} \lesssim 30$ s. We thus see that as soon as dust sublimation is initiated, the dust coma that has been extending around the FEB during its apoastron passage is immediately blown away by dust sublimation and reduced to virtually nothing if present. This justifies the fact that we neglected dust in our simulations.

## 7. Influence of parameters

The results presented above concern a given set of initial parameters. We investigate now the sensitivity to these parameters. They can be classified into two subsets: dynamical and physical (intrinsic) parameters. We recall here that the default parameters for the sublimations presented below, apart from specific changes, are listed in Table 1.

### 7.1. Dynamical parameters

The quicker the evolution of the eccentricity, the smaller is the number of orbits required to reach close periastron values. Therefore we expect a quicker eccentricity growth to allow it to reach smaller periastron values, and so better explains HVFs.

Many dynamical parameters may influence the eccentricity growth. Here we investigate the mass of the perturbating planet, the eccentricity of the perturbating planet, the order of the resonance, and the initial eccentricity of the object.

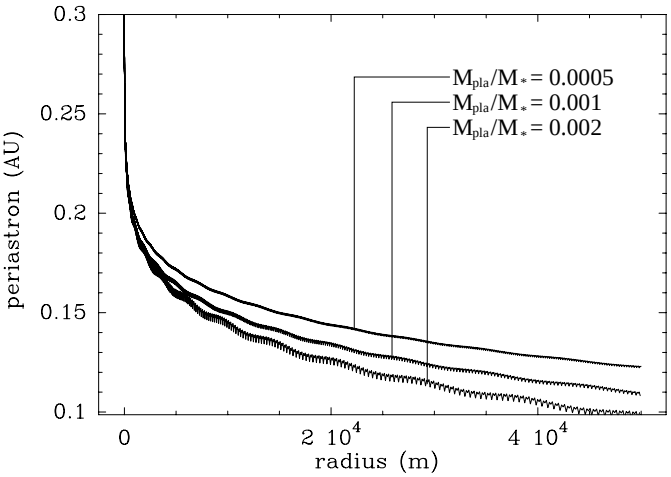


**Fig. 9.** Minimum periastron that FEBs can reach, versus their size, for values of $\mu$ of (from top to bottom) 0.0005, 0.001 and 0.002.

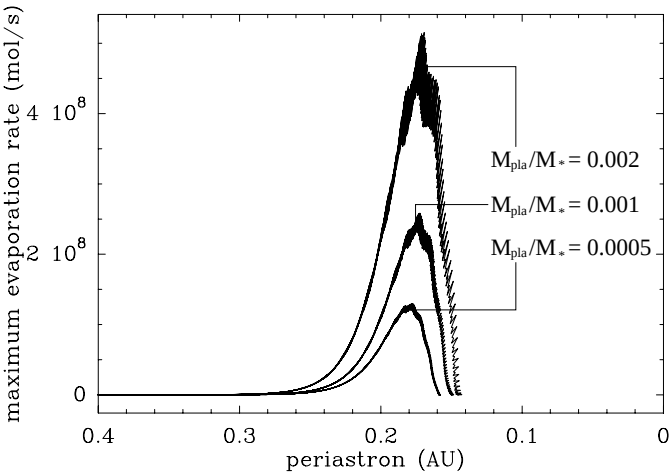


**Fig. 10.** Rate of refractory matter sublimation at each periastron passage, versus the distance at the periastron for values of $\mu$ of (from top to bottom) 0.002, 0.001 and 0.0005.

### 7.1.1. The mass of the planet

The mass of the planet is represented in the dynamical model by $\mu$, the ratio of the mass of the planet to the mass of the star. Typically, we consider that the planet has a mass of the order of Jupiter, therefore $\mu \simeq 0.001$. Figure 9 shows the periastron where the object disappears definitively versus the radius of the object. Figure 10 shows the quantity of refractories sublimated at each periastron passage. As expected, a more massive planet speeds the secular evolution of the FEB, and allows it to reach smaller periastron distances. We can see that the minimum periastron is relatively small, between 0.1 AU and 0.125 AU. However, the rate of sublimation of matter is far higher with a massive planet.

### 7.1.2. The eccentricity of the planet

The eccentricity of the planet also influences the efficiency of the penetration in the sublimation area. Figure 11 shows the sublimation rate for different eccentricities. The difference

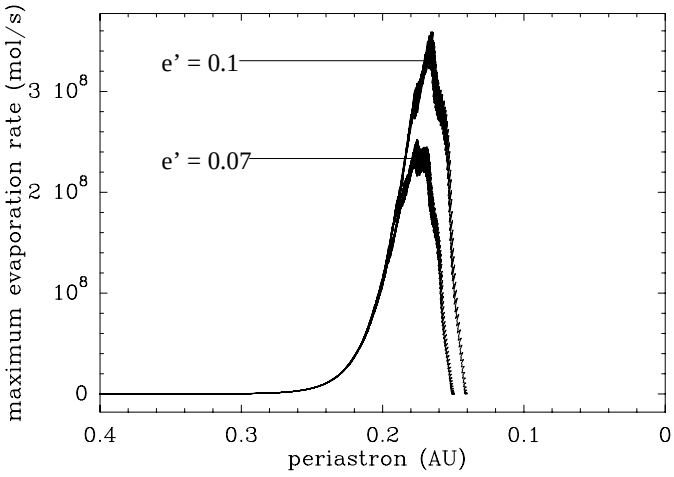


**Fig. 11.** Quantity of refractory matter sublimated per second at each periastron passage, versus the periastron distance, for eccentricity values of (from top to bottom) 0.1 et 0.07. Recall that the dynamical process that brings the eccentricity up to 1 is only active for $e' \gtrsim 0.05$ (Beust & Morbidelli 2000).

exists, but is not as large. It only allows the FEB to approach a little closer to the star.

### 7.1.3. The initial eccentricity of the object

Some tests have been done with an initial eccentricity of 0.05 and of 0.1. The results show no difference. The growth of eccentricity occurs earlier for a higher eccentricity, but the end of the evolution, i.e. the FEB phase, remains unchanged.

### 7.1.4. The 3:1 resonance

The 3:1 resonance is more efficient in some circumstances, when the object has a high initial eccentricity. With an eccentricity of 0.2 and an eccentricity of the planet of 0.1, the dynamical evolution is very fast. Some recent work suggests that the dominant mechanism to create FEBs should be this, instead of 4:1 resonance (Thébault & Beust 2001). Figure 12 compares the results obtained previously with the 4:1 resonance and the results obtained in the same conditions but for a body trapped in the 3:1 resonance. We observe a stronger ability to penetrate deep in the sublimation area, due to the quickness of the dynamical evolution of the object in the 3:1 resonance. The objects contained in this resonance are therefore more able to generate the HVF features.

## *7.2. Physical parameters*

The physical parameters are the values that influence the quantity of refractory matter sublimated, the total quantity of matter present in the object, or the propagation of heat and gas in the interior.

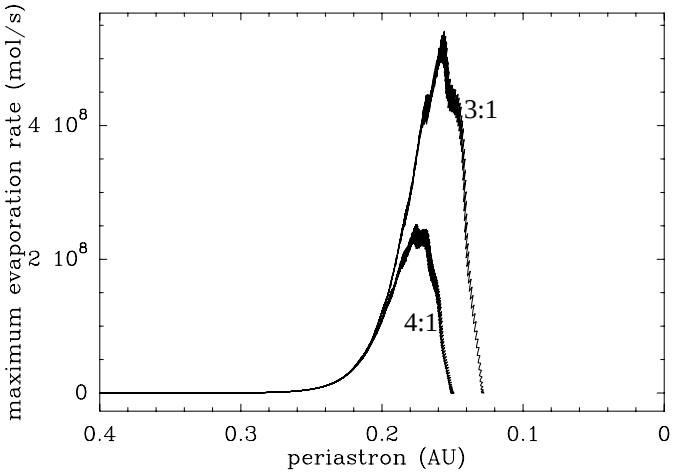


**Fig. 12.** Maximum quantity of refractory matter evaporated per second at each periastron, versus the distance at the periastron, for (from top to bottom) the 3:1 and 4:1 resonances. See the text for precise parameters.

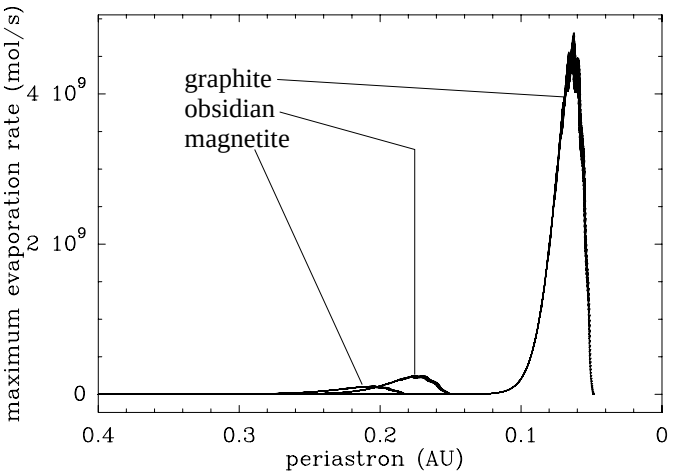


**Fig. 13.** Quantity of refractory matter sublimated by second at each periastron, versus the distance at periastron, for (from left to right) magnetite, obsidian, and graphite.

### 7.2.1. The refractory material

We do not know much about the refractory material contained in the FEB. The choice of obsidian was made to mimic what is observed on an average in the Solar System (Draine & Lee 1984). But the possible refractory materials are still various, and can show a great diversity of physical properties. If obsidian is a good average, we have also simulated some other materials: magnetite, which sublimates very easily, and graphite, which is very hard to sublimate.

The results are shown in Fig. 13. We observe that as graphite is tougher than the other materials it is allowed to approach very close to the star. The main part of its sublimation takes place between 0.1 AU and 0.05 AU. Therefore, one could think that a FEB composed essentially of carbon or being at least strongly carbonaceous is less likely to produce the low velocity features (LVF or VLVF) observed. On the other hand, it is apparently the only material able to produce high velocity features, and it does so very efficiently. This result is very important as it is the first convincing evidence of the fact that physically different objects produce very different features. In this scenario, a wide variety of objects is necessary to produce the variety of the features.

This is to be crosschecked with the observations of the carbon element (in the form of CO, C I or C IV) in the absorption features, that shows that this element seems to appear mostly in high velocity features (HVF). Nevertheless, we cannot exclude an observational bias, as the carbon is detected in the far UV.

Magnetite, which is less tough, sublimates far from the star, and its sublimation is smoother. Obsidian is a material somewhat close to magnetite. These kind of materials are therefore those expected in FEBs that produce LVFs and VLVFs features.

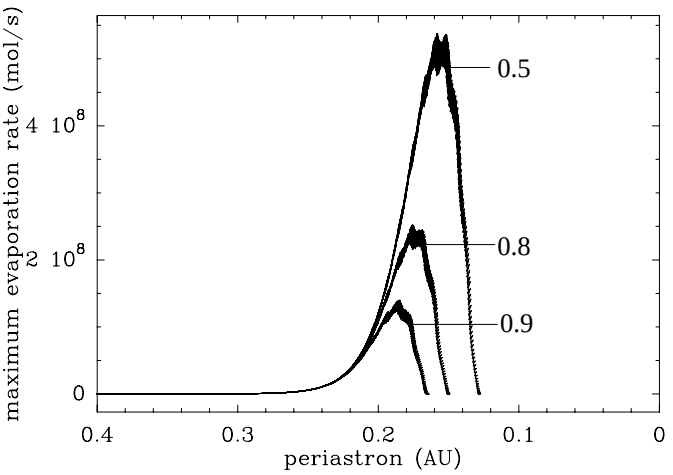


**Fig. 14.** Rate of refractory matter sublimation at each periastron, versus the distance to the star at the periastron, for porosity values of (from top to bottom) 0.5, 0.8 and 0.9.

### 7.2.2. Porosity

The porosity influences the quantity of matter inside the object. If there is more matter for a constant sublimation rate the size of the object will decrease slower.

Figure 14 shows the effect of porosity. We see, as expected, that lower porosity induces higher sublimation rates and allows the FEB to reach closer periastrons. The effect is somewhat important, even with a moderate porosity (0.5).

## *7.3. Complete sublimation?*

The evolution of eccentricity in a mean-motion resonance is theoretically a periodical phenomenon; an object after having passed through a maximum of eccentricity evolves secularly back towards a nearly circular orbit, at which point a new cycle starts again. However, the simulations show that reasonably-sized objects cannot resist sufficiently long to live a whole cycle. It is even very difficult for them to reach the maximum excentricity allowed by the dynamics. Only objects that have a size of the order of $10^3$ km or more can do it. Objects of that type are not realistic, and should be very unusual.

This might explain the limited number of blue-shifted events. They may correspond in the $\beta$ Pic dynamic conditions

to objects that have reached this maximum of eccentricity, and that have taken the inverse way of the secular dynamical evolution. For example, for the 4:1 resonance, a compact object (porosity = 0) should have a radius of 1500 km to pass this maximum. For the 3:1 resonance, which induces a faster dynamical evolution, a radius of 300 km should be "sufficient".

## 8. Consequences for the FEB sublimation model and observations

In K01, the conclusion of the possible absence of an icy core led to the idea that the FEB evaporation model needed to be revised in order to handle the lack of volatiles materials. This time, the simulations of the FEB evolution describes a complete scenario of the evaporation sequences that will have to be introduced in this evaporation model.

The quantity and the nature of the matter sublimated when the object enters the refractory sublimation limit probably have a direct effect on the observed absorption features. Indeed it can be observed only if the object develops a large and dense enough coma of metallic material, and the quantity of matter evaporated as well as the respective proportion of refractory and volatile material in this evaporation can have effects on the development of the cloud. In order to fulfill this requirement, the material escaping from the nucleus must be produced in sufficiently high quantities and must contain some species undergoing very little radiation pressure. Most of the spectral lines exhibiting FEB variable components concern metallic species that undergo a high radiation pressure (Lagrange et al. 1998). When released by the body, these ions are immediately subject to the stellar radiation pressure, so that if nothing else is able to retain them, they are blown away and the resulting coma is too thin to be detectable. If the ions encounter a dense enough medium that does not suffer from a strong radiation pressure, then collisions can prevent them from being too quickly blown away, and a large coma forms (Beust et al. 1996). Volatiles have historically been candidates for this role, as they suffer very little radiation pressure (Lagrange et al. 1998), but it is not so clear: some refractory species can also do the job. Therefore the simulations of this paper are very important as they show the respective amount of refractory and volatile matter really evaporated by an object.

The scenario drawn here involves many situations. First, an object in the phase described in Sect. 4 that still has a refractory crust will have a highly predominant refractory evaporation, with very little volatile evaporation. At this time, the effect of volatiles in the formation of the cloud is highly questionable. In the following phase, which is the last one, described in Sect. 5, the ratio between refractory and volatile evaporation is highly variable, and a very important point is the evolution of the productions rates of the object when it crosses the line of sight, and before. First, it evaporates mainly refractory materials, and a few volatiles, then if it crosses the line of sight at this time, the cloud will be dominated by ions originating from refractory matter (mainly metallic ions, but also C and 0 ions). Then the crust disappears and the rates of refractory and volatile matter become equivalent. At this point, we could say that the cloud is full of matter of both sources but it is not so clear, as ions of volatiles origin enter in a medium filled with ions of refractory origin, and then may take some time to be important in the cloud formation process. At last, the volatile production is predominant, and we can expect the cloud to be progressively filled by ions of volatile origin. As we can see, the process of cloud formation can be very complex in the later phase and it will have to be fully investigated with dedicated simulations in the future. Notice that the case when the volatiles are predominant may only occur at the end of the passage at the periastron, so "volatile-born" clouds crossing the line of sight should occur only for blue-shifted events, which are not often observed. It may be another explanation for the lack of observations of blue-shifted events around $\beta$ Pictoris and in other systems: if the cloud after the passage to the periastron is dominated by some H I or H II gas, the physics inside the cloud would be dominated by those ions, which do not undergo stellar radiation, and the cloud would have great difficulties in developing, as stated before. It is another issue that should be investigated in a future complete study of the cloud. Then, the last point of importance is the influence of the chemical composition of the objects themselves on the events. It is impossible for a unique type of object to produce all the FEB events observed, and therefore detailed observations of those events should show strong differences in the species of the ions observed if they are HVFs, LVFs or VLVFs. Especially, carbonaceous objects are expected to be the progenitors of HVF, and those events should then show C I, C IV and other carbon ions (as it seems indeed to be the case).

However, it does not mean that more fragile materials are not capable of appearing in HVFs. Just as the ice can succeed in staying in FEBs until complete evaporation because of the formation of a refractory crust, fragile refractory materials such as obsidian can resist under a crust of tough materials, which would possibly form at distances between 0.4 and 0.1 AU. In this scenario, we would have a three-layer description of a body with a crust of tough refractory materials involving probably carbon, an underlying mantle of fragile refractory materials such as obsidian, mixed with tough materials, and a possible icy core. This kind of object would certainly show the same kind of "season effect" developed here, but it is beyond the scope of our model.

## 9. Conclusion

In order to simulate the physico-chemical evolution of the FEB during evaporation, we have developed the model presented in K01 to take into account the sublimation of refractory materials and the dynamical evolution. We have also optimized the numerical resolution by grouping the spatial intervals. Many important elements have emerged from these studies. First, it turns out that the crust of refractory materials finally disappears before the icy core. Then, we observe a season effect at passages to the periastron: there is a time-shift between the production of volatiles and the production of refractory gas, due to the formation of a small crust between two passages. The production of the object is subject to the influence of the periastron value and the moment of the passage to the periastron during which it crosses the line of sight. The rate of the

sublimation leads to the idea that all kind of FEB features cannot be produced by the same kind of objects, and that the FEB population is probably very heterogeneous, especially for the kind of refractory materials that are predominant in their composition.

*Acknowledgements.* All the computations presented in this paper were performed at the Service Commun de Calcul Intensif de l'Observatoire de Grenoble (SCCI).

## References

Artymovicz, P. 1997, Ann. Rev. Earth Planet. Sci., 25, 175
Beust, H., Lagrange-Henri, A.-M., Vidal-Madjar, A., & Ferlet, R. 1990, A&A, 236, 202
Beust, H., Lagrange, A.-M., Plazy, F., & Mouillet, D. 1996, A&A, 310, 181
Beust, H., & Morbidelli, A. 1996, Icarus, 120, 358
Beust, H., Lagrange, A.-M., Crawford, I. A., Goudard, C., & Spyromilio, J. 1998, A&A, 338, 1015
Beust, H., Lagrange, A.-M., Crawford, I. A., et al. 1998, A&A, 338, 1015
Beust, H., & Morbidelli, A. 2000, Icarus, 143, 170
Dean, J. A. 1985, in Lange's handbook of chemistry (McGraw-Hill)
Draine, B. T., & Lee, H. M. 1984, AJ, 285, 89
Douglas, J., & Jones, B. F. 1963, Soc. Ind. and App. Math. Jour., 11(1), 195
Espinasse, S., Klinger, J., Ritz, C., & Schmitt, B. 1989, International Workshop on Physics and Mechanics of Cometary Materials, 185
Espinasse, S., Klinger, J., Ritz, C., & Schmitt, B. 1991, Icarus, 92, 350
Karmann, C., Beust, H., & Klinger, J. 2001, A&A, 372, 616
Lagrange, A.-M., Plazy, F., Beust, H., et al. 1996, A&A, 310, 547
Lagrange, A.-M., Beust, H., Mouillet, D., et al. 1998, A&A, 330, 1091
Lagrange, A.-M., Backman, D. E., & Artymovics, P. 2000, Planetary Material around Main Sequence Stars, in Protostars and Planets IV, ed. V. Mannings, A. P. Boss, & S. S. Russell (Tucson: University of Arizona Press)
Lamy, P. L. 1974, A&A, 35, 197
Mukai, T., & Schwehm, G. 1981, A&A, 95, 373
Smith, B., & Terrile, R. 1984, Science, 226, 1421
Spohn, T., Seiferlin, K., & Benkhoff, J. 1989, in Thermal conductivities and diffusivities of porous ice samples at low pressures and temperatures and possible modes of heat transfer in near surface layers of comets, ed. J. Hunt, T. D Guyenne, Physics and Mechanics of Cometary Materials, ESA SP-302, 77
Tancredi, G., Rickman, H., & Greenberg, J. M. 1994, A&A, 286, 659
Thébault, P., & Beust, H. 2001, A&A, 376, 621
Vidal-Madjar, A., Lagrange-Henri, A.-M., Feldman, P. D., et al. 1994, A&A, 290, 245
Vidal-Madjar, A., Lecavelier des Etangs, A., & Ferlet, R. 1998, Planet. Space Sci., 46, 629